Available online at www.sciencedirect.com
SCIENCE DIRECT
Journal of Power Sources 153 (2006) 391–395
JOURNAL OF POWER SOURCES
www.elsevier.com/locate/jpowsour

Short communication

Electrochemical impedance spectroscopy study of the SEI formation on graphite and metal electrodes

H. Schranzhofer [a], J. Bugajski [a], H.J. Santner [b], C. Korepp [b], K.-C. Möller [b], J.O. Besenhard [b], M. Winter [b], W. Sitte [a,*]

[a] *Department of General, Analytical and Physical Chemistry, University of Leoben, A-8700 Leoben, Austria*
[b] *Institute for Chemical Technology of Inorganic Materials, Graz University of Technology, A-8010 Graz, Austria*

Available online 9 August 2005

Abstract

The long-term formation kinetics of the solid electrolyte interphase (SEI) was studied on graphite electrodes in 1 M $LiClO_4$/PC with 5% acrylonitrile (AN) as electrolyte additive by electrochemical impedance spectroscopy at 1.0 and 0.5 V versus Li/Li^+, i.e. mainly outside the graphite intercalation region. To support the interpretation of the results, comparative experiments with Ni and Pt electrodes were performed at the same potentials. The resistance of the SEI on graphite and nickel shows similar time dependence. Whereas, R_{SEI} of both electrodes exhibits a linear increase after 5–10 h at 1.0 V, a parabolic behavior could be observed at 0.5 V (and even more expressed for Ni at 0.05 V) typical of diffusion controlled growth kinetics. Temperature dependent measurements yielded activation energies for the ionic conduction of the SEI between 0.61 and 0.66 eV. The results were the same for graphite at 0.5 V and nickel at 1.0, 0.5 and 0.05 V.

Keywords: SEI; Li-ion cells; Impedance spectroscopy; Graphite; Nickel; Platinum

1. Introduction

Lithium ion batteries are now commercially used in a wide range of applications but research is still going on mainly to improve efficiency, safety, lifetime and production costs [1,2]. To improve cell performance, different materials for the working and counter electrode as well as for the electrolyte are investigated. Liquid electrolytes regularly used are mixtures of aprotic organic solvents with lithium salts such as $LiPF_6$ or $LiClO_4$. The cells operate in a wide electrochemical potential window (0.0–4.5 V versus Li/Li^+), which is beyond the thermodynamic stability limits of the organic electrolyte. Therefore, the electrolyte is oxidized and reduced at cathode and anode, respectively. This electrolyte decomposition does proceed mainly, but not exclusively during the first charging process. In the best case, the decomposition products form a film on the electrode surface.

Ideally, this solid electrolyte interphase (SEI) [3] film is regarded as a new phase with the function of a solid electrolyte for lithium ions, but as insulator for other charged (electrons, anions, solvated lithium cations) or neutral (electrolyte solvents, impurities) species. To influence the electrochemical behavior small amounts of certain electrolyte additives are used, e.g. [4,5]. One of the reasons to use additives is to influence the solid electrolyte interphase (SEI) formation on the working electrode. This formation process takes place mainly in the first charging cycle and leads to a high irreversible charge value. Nevertheless, this SEI is necessary for a correct operation of the electrochemical system. In the case of $LiClO_4$ in propylene carbonate (PC) with graphite as a working electrode the SEI prevents PC co-intercalation into the graphite layers, what would lead to high volume expansion and furthermore to the destruction of the working electrode. Also, the reduction products of PC (mainly propene gas) further cause the shedding of single graphene layers [5]. This solvated intercalation usually starts at electrode potentials of 1.0–0.9 V versus Li/Li^+. So the aim is to find an additive, which is reduced at higher potentials than PC. In this study,

* Corresponding author.
E-mail address: sitte@unileoben.ac.at (W. Sitte).

0378-7753/$ – see front matter © 2005 Published by Elsevier B.V.
doi:10.1016/j.jpowsour.2005.05.034

acrylonitrile (AN) was chosen which initiates a SEI formation at a potential of approximately 1.3 V versus Li/Li^+ at graphite and therewith avoids PC reduction and solvent co-intercalation [6].

Due to their usually porous structure graphite electrodes show a complex impedance behavior, which has been treated by numerous models in the past [7–11]. It was the aim of this paper to investigate the SEI formation kinetics on graphite and to compare the results with those from pure metal electrodes [12] with geometrically defined surfaces. Our studies concentrated on the solid electrolyte interphase by fitting the high frequency part of the impedance spectra to a single depressed semicircle. The impedance spectra were taken at potentials where no Li intercalation into graphite occurs. To elucidate general trends the results from the graphite electrode have been compared with those from the pure metal electrodes.

2. Experimental

The electrolyte (1 M $LiClO_4$/PC + 5 vol% AN) and the graphite electrodes (TIMREX® SFG44 with 4 wt.% PVdF binder) were prepared as described in [6]. This as well as the assembling of the glass cell was done in a glove box. The cell was hermetically sealed and all experiments were then performed outside the glove box.

The nickel electrode (Aldrich, 99.98%, 0.1 mm thickness) and the platinum electrode (Ögussa, 99.9%, 0.1 mm thickness) had both the same geometry as the graphite electrodes (5 mm × 5 mm, on both sides in contact with the electrolyte). The metal electrodes were re-used after polishing with diamond paste (1 μm), cleaning with H_2O and acetone and drying under vacuum for at least 12 h.

Pure lithium foils served as counter electrodes (CE), which were placed symmetrically on both sides of the working electrode (WE) (graphite or metal electrode) allowing a symmetric current flow. A lithium reference electrode (RE) was placed close to the WE. All electrodes were fixed on stainless steel holders, which were connected to BNC cables.

Impedance measurements were performed using a frequency response analyzer (Solartron 1260) in combination with an electrochemical interface (Solartron 1286). The instruments were connected via GPIB interface to a computer and controlled by ZPlot and CorrWare (Scribner Associates).

The conditions for the experiments were as follows: at the beginning, the potential was kept constant at 2.0 V versus Li/Li^+ for 30 min. Then, a potentiodynamic loading step of 100 μV s^{-1} followed, until the desired potential was reached (1.0, 0.5 or 0.05 V). This potential was kept constant for the next 60 h. The first impedance spectrum was taken immediately after the desired potential has been reached, the other spectra every 2 h for the next 60 h. All measurements were performed within a frequency range from 600 kHz to 0.5 Hz and with an amplitude of 10 mV. During the whole experiments the cell was kept at 20.0 °C by the use of a thermostat (Lauda RC 6). The impedance spectra were fitted using the simple 'fit circle' routine of Zview. This routine delivered a resistance calculated from the difference between the high and low intercept of the fitted semicircle and a capacity by using the relationship $\omega_{max} = 1/(RC)$, wherein ω_{max} is the angular frequency of the maximum of the fitted semicircle. Evaluations with different models from literature, e.g. [8,9,12–14], did not indicate any significant differences with respect to the qualitative conclusions we draw within this study. Nevertheless, details regarding the application of various models for data evaluation will be published in a separate study [15].

The temperature dependent measurements were performed as follows: after 60 h the cell was allowed to stand for another 12 h under OCV conditions at 20.0 °C. Impedance spectra were taken at 20.0, 12.0 and 4.0 °C and again at 12 and 20 °C. At each temperature the cell reached thermal equilibrium within approximately 30 min.

3. Results and discussion

Fig. 1 shows the charge curves for the graphite (SFG44, 0.725 mg) and the platinum electrode (0.5 cm^2). The peaks at approximately 1.2 V for graphite and at approximately 1.7 V for platinum indicate the reduction of the electrolyte additive acrylonitrile (AN) and the consecutive formation of the SEI during potentiodynamic charging. Due to the small surface area of the Ni electrode (0.5 cm^2) only small currents below 1 μA flow (not displayed).

For the investigations of the SEI formation kinetics the potentials 1.0 and 0.5 V versus Li/Li^+ were chosen. These potentials are below the SEI formation on graphite as well as those of Ni or Pt and no remarkable lithium intercalation into graphite occurs between 0.5 and 1.0 V versus Li/Li^+. Additionally, Pt reacts with lithium at potentials below 0.2 V versus Li/Li^+, and therefore Ni was used for additional investigations at 0.05 V versus Li/Li^+.

Fig. 2 shows typical impedance spectra of the nickel electrode at 0.5 V. The increase of the high frequency depressed semicircles within the first 60 h reflects the increase of the resistance of the electrode due to the SEI formation. From detailed investigations of the surface area by chemisorption of methylene blue [15] we estimate the active surface of our graphite electrode (TIMREX® SFG44 with 4 wt.% PVdF binder) to about 5 cm^2 mg^{-1}. In comparison, the binder-free graphite powder has a BET surface area of 50 cm^2 mg^{-1} [16].

In Fig. 3, the time dependence of the resistance of the graphite electrode due to the SEI formation is presented. The high frequency part of the impedance spectra at 0.5 and 1.0 V was fitted to a single depressed semicircle.

Whereas, the R_{SEI} values at 0.5 V show a weak parabolic like behavior, the values for 1.0 V are decreasing for the first 10–15 h and then increasing almost linearly. It should be mentioned that R_{SEI} at 1.0 V may well include the resistance of the charge transfer process (the ion transfer from the electrolyte

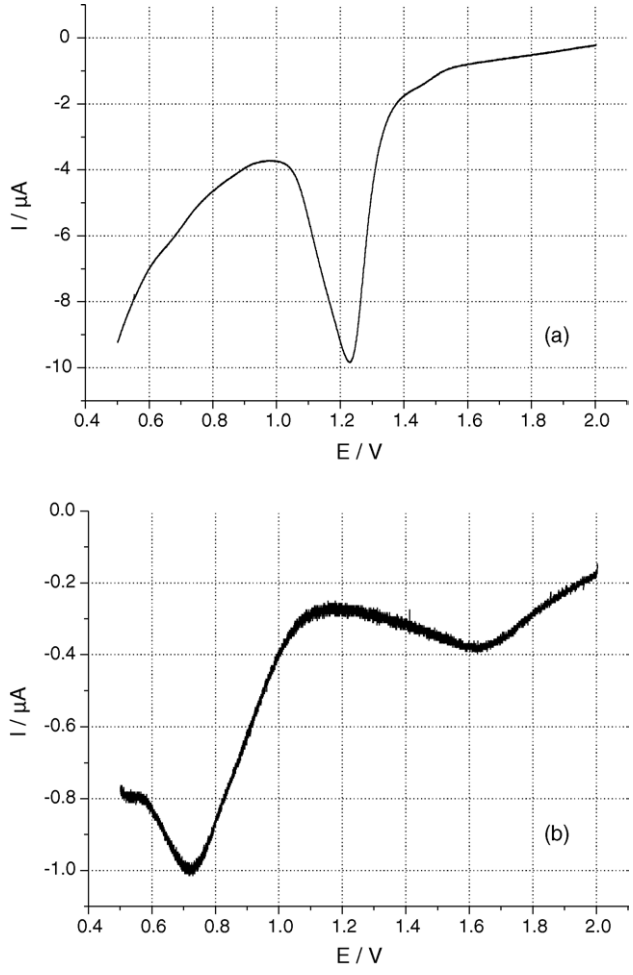

Fig. 1. Charge curves of the graphite (TIMREX® SFG44 with 4 wt.% PVdF binder) (a) and platinum (0.5 cm^2) (b) (scanrate 100 $\mu V\,s^{-1}$). The peaks at approximately 1.2 V for graphite and at 1.7 for platinum indicate the reduction of the additive AN and the consecutive formation of the SEI.

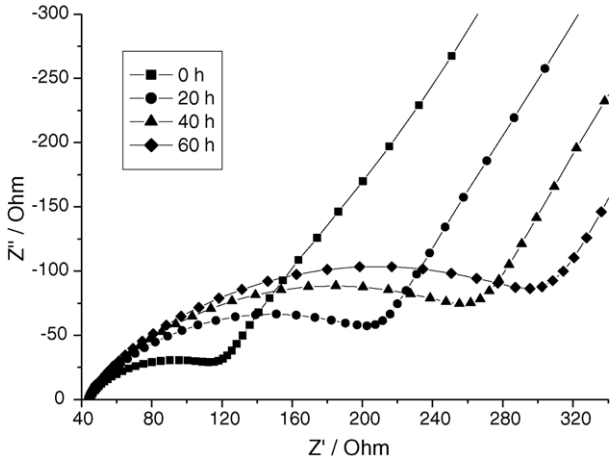

Fig. 2. Time development of the impedance spectra of the nickel electrode at 0.5 V. The increase of the high frequency depressed semicircles with time (between 0 and 60 h) reflects the increase of the resistance of the graphite electrode due to the SEI formation (the curves are a guide to the eye).

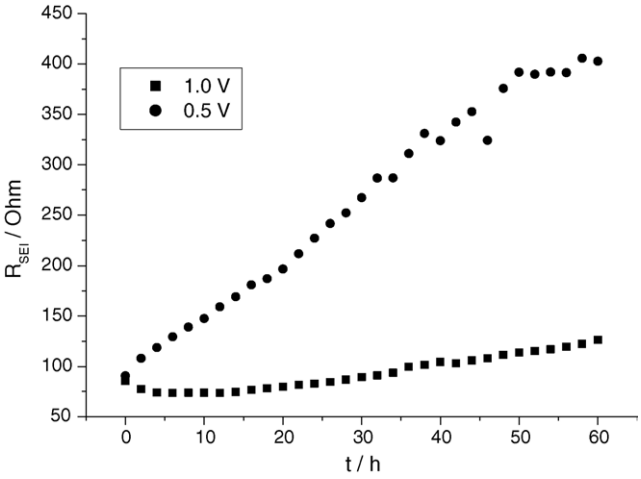

Fig. 3. Time dependence of R_{SEI} of the graphite electrode.

into the SEI) as could be detected by the lower activation energy of the ionic transport. We do not expect the charge-transfer resistance to vary significantly with time at these constant potentials and therefore the SEI formation kinetics obtained for the graphite electrode at 1.0 and 0.5 V may be extracted at least qualitatively.

Fig. 4 shows the time development of R_{SEI} at the platinum and nickel electrode at 1.0 and 0.5 V. For nickel also the values for 0.05 V are included, as nickel—in contrast to platinum—does not react with lithium at this potential.

As an important conclusion from Fig. 4 we see that the time dependence of R_{SEI} is very similar for Ni and Pt electrodes. A parabolic increase of the SEI-resistance can be observed at 0.5 V for both electrodes as well as at 0.05 V for the nickel electrode, which we attribute to the increased electronic conductivity of the SEI at these lithium activities with increased chemical diffusion of lithium. The almost linear

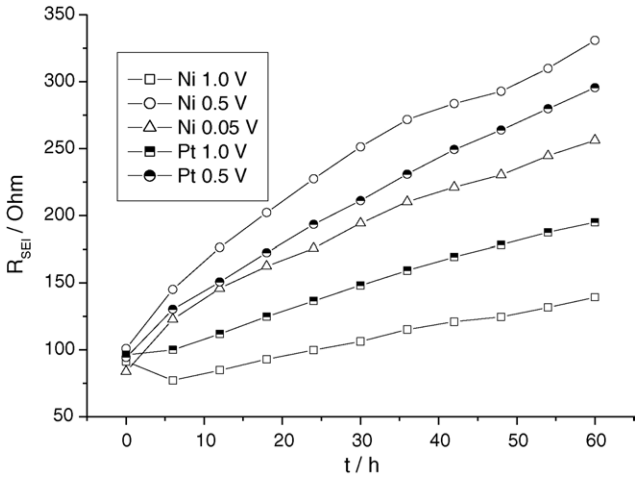

Fig. 4. Time dependence of R_{SEI} of the Ni and Pt electrodes at 0.5 and 1.0 V. For nickel also the values for 0.05 V are included.

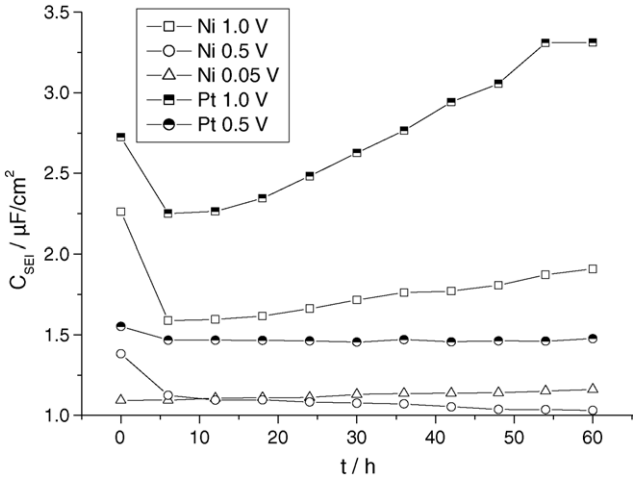

Fig. 5. Time development of C_{SEI} of the Ni and Pt electrode at 1.0 and 0.5 V. For nickel also the values for 0.05 V are included.

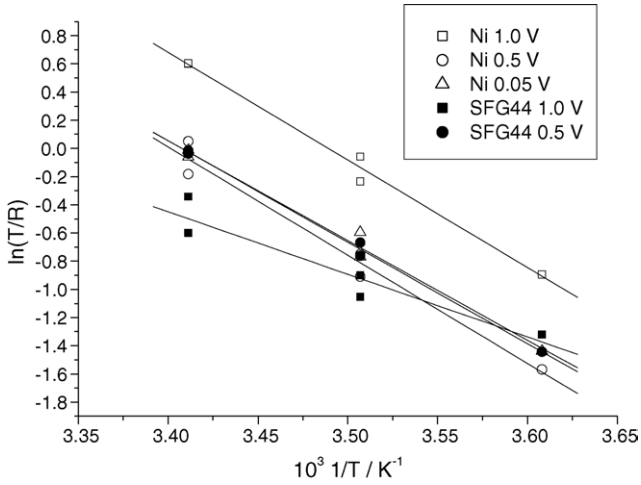

Fig. 7. Arrhenius plot for graphite and Ni at 1.0 and 0.5 V as obtained from the R_{SEI} values from the depressed high-frequency semicircle. For nickel also the values for 0.05 V are included.

increase found at 1.0 V for Ni and Pt could be assigned to the slow growth of the primarily ionic SEI. The behavior at 1.0 and 0.5 V can well be compared with that of graphite (Fig. 8).

The capacities resulting from the fitting procedure for both electrodes are shown in Fig. 5 and are in the order of magnitude of 1 $\mu F\,cm^{-2}$ as usually assumed for the solid SEI in the literature [12]. Whereas, the time dependence of the capacity can well be understood for 0.5 V for Pt and Ni and also for 0.05 V for Ni (the capacity is decreasing with increasing film thickness), we see an increase of C_{SEI} after about 10 h for both electrodes at 1.0 V. This behavior may be attributed to a variation of the structure of the SEI (due to e.g. a slow recrystallisation process).

The time dependence of the depression angle of the fitted depressed semicircle is shown in Fig. 6 for both metal electrodes. The most distinct changes in the depression angle occur within approximately the first 15 h, which indicates a change of the SEI structure [17] during its initial growth period.

In order to obtain the activation energy for the ionic conduction of the SEI we performed temperature dependent measurements after the SEI has formed after 60 h. R_{SEI} values as obtained at 4, 12, and 20 °C (each measured after short thermal equilibration for about 30 min) were used for the Arrhenius plots (Fig. 7). From these plots the activation energies for the ionic conduction were calculated as follows: E_a(graphite, 1.0 V) = 0.38 eV, E_a(Ni, 1.0 V) = 0.66 eV, E_a(graphite, 0.5 V) = 0.62 eV, E_a(Ni, 0.5 V) = 0.66 eV, E_a(Ni, 0.05 V) = 0.61 eV. Thus, very similar activation energies for graphite and nickel at 0.5 V and for nickel at 0.05 V result.

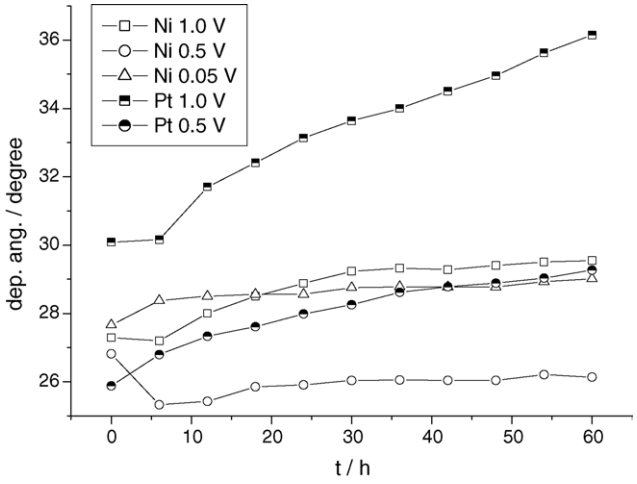

Fig. 6. Time dependence of the depression angle for Ni and Pt at 1.0 and 0.5 V. For nickel also the values for 0.05 V are included.

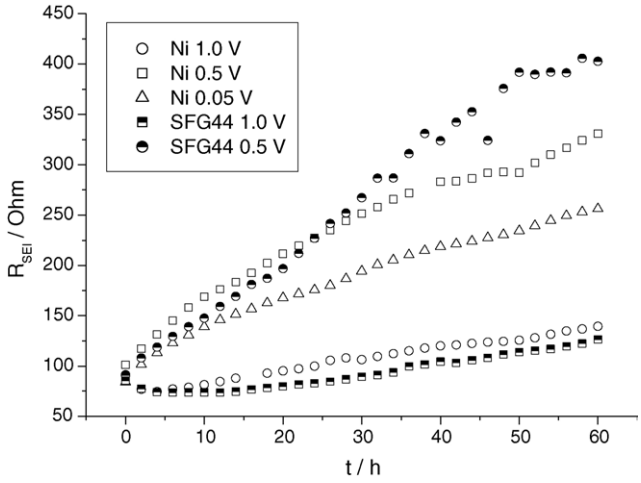

Fig. 8. Comparison of the time development of the R_{SEI} for graphite and nickel at 1.0 and 0.5 V. For nickel also the values for 0.05 V are included.

These values can be compared with that of graphite at 0.16 V (E_a = 0.58 eV) [7]. (For comparison the temperature dependence of the resistance of the liquid electrolyte delivered a totally different 'activation energy' of only 0.08 eV, but we are aware of the fact that due to the different behavior of liquid electrolytes this value has no physical meaning).

Fig. 8 compares the time dependence of R_{SEI} for the graphite and nickel electrodes at 1.0 and 0.5 V, showing indeed similar behavior of both electrodes. Whereas, the time dependence of R_{SEI} of both electrodes shows a linear increase after 5–10 h, the behavior at 0.5 V (and even more expressed for Ni at 0.05 V) can be understood by a parabolic behavior typical of diffusion controlled growth kinetics.

4. Conclusions

Our studies concentrated on the solid electrolyte interphase by fitting the impedance spectra to a depressed high frequency semicircle. To elucidate general trends the results have been compared with those from pure metal electrodes. While qualitative conclusions can be drawn from this procedure, it should be kept in mind that alternative evaluation techniques with further experiments are needed for more quantitative descriptions. Ni and Pt electrodes with geometrically defined surfaces helped to understand the SEI formation kinetics on the graphite electrode at various potentials, although detailed investigations presently end up with the problem that the exact surface of the graphite electrode in contact with the liquid electrolyte is not known.

Acknowledgment

Support by the Austrian Science Funds through the special research program Electroactive Materials (projects F911 and F915) is gratefully acknowledged.

References

[1] J.O. Besenhard (Ed.), Handbook of Battery Materials, Wiley-VCH, 1999.
[2] W.A. van Schalkwijk, B. Scrosati, Advances in Lithium-Ion Batteries, Kluwer Academic/Plenum Publishers, 2002.
[3] E. Peled, J. Electrochem. Soc. 126 (1979) 2047.
[4] G.H. Wrodnigg, J.O. Besenhard, M. Winter, J. Electrochem. Soc. 146 (1999) 470.
[5] M. Winter, W.K. Appel, B. Evers, T. Hodal, K.-C. Möller, I. Schneider, M. Wachtler, M.R. Wagner, G.H. Wrodnigg, J.O. Besenhard, Chemical Monthly 132 (2001) 473.
[6] H.J. Santner, K.-C. Möller, J. Ivanco, M.G. Ramsey, F.P. Netzer, S. Yamaguchi, J.O. Besenhard, M. Winter, J. Power Sources 119–121 (2003) 368.
[7] M.D. Levi, C. Wang, D. Aurbach, J. Electrochem. Soc. 151 (2004) A781.
[8] C. Wang, A.J. Appleby, F.E. Little, Electrochim. Acta 46 (2001) 1793.
[9] R. Yazami, Y.F. Reynier, Electrochim. Acta 47 (2002) 1217.
[10] Y.-O. Kim, S.-M. Park, J. Electrochem. Soc. 148 (2001) 194.
[11] B. Markovsky, M.D. Levi, D. Aurbach, Electrochim. Acta 43 (1998) 2287.
[12] A. Zaban, D. Aurbach, J. Power Sources 54 (1995) 289.
[13] D. Aurbach, A. Zaban, J. Electroanal. Chem. 367 (1994) 15.
[14] M. Holzapfel, A. Martinent, F. Alloin, B. Le Gorrec, R. Yazami, C. Montella, J. Electroanal. Chem. 546 (2003) 41.
[15] H. Schranzhofer et al., to be published.
[16] http://www.timcal.com/html/corpo/products/pdf_doc/sfg44.pdf.
[17] D. Aurbach, A. Zaban, J. Electroanal. Chem. 348 (1993) 155.